The JEM-EUSO mission – Instrument

N. Sakaki[a,4], T. Ebisuzaki[1], K. Maekawa[1], H. Ohmori[1], Y. Kawasaki[1], Y. Takizawa[1], K. Katahira[1], S. Wada[1], K. Kawai[1], H. Mase[1], K. Shinozaki[1], Y. Yazu[1], F. Kajino[2], M. Sakata[2], H. Sato[2], T. Yamamoto[2], Y. Yamamoto[2], N. Ebizuka[2], M. Nagano[3], Y. Miyazaki[3], T. Shibata[4], N. Inoue[5], Y. Uchihori[6], K. Nomoto[7], Yu. Takahashi[8], M. Takeda[9], Y. Arai[10], Y. Kurihara[10], H.M. Shimizu[10], J. Fujimoto[10], S. Yoshida[11], K. Mase[11], Y. Mizumoto[12], J. Watanabe[12], T. Kajino[12], K. Asano[13], H. Ikeda[14], M. Suzuki[14], T. Yano[14], T. Murakami[15], D. Yonetoku[15], N. Sugiyama[16], Y. Itow[17], S. Nagataki[18], S. Inoue[19], A. Saito[19], S. Abe[20], M. Nagata[20], T. Tajima[21], M. Chikawa[22], M. Tajima[23], M. Sato[24], J. H. Adams Jr.[25], S. Mitchell[25], M.J. Christl[25], J. Watts Jr.[25], A. English[25], R. Young[25], Yo. Takahashi[26], V. Connaughton[26], D. Gregory[26], M. Bonamente[26], K. Pitalo[26], J. Hadaway[26], J. Geary[26], R. Lindquist[26], P. Reardon[26], T. Blackwell[26], H. Crawford[27], E. Judd[27], C. Pennypacker[27], K. Arisaka[28], D. Cline[28], V. Andreev[28], A. Berlind[29], T. Weiler[29], S. Csorna[29], R. Chipman[30], S. McClain[30], J-N. Capdevielle[31], P. Gorodetzky[31], D.Allard[31], J. Dolbeau[31], J.J. Jaeger[31], E. Parizot[31], T. Patzak[31], D. Semikoz[31], J. Weisbard[31], M. Teshima[32], T. Schweizer[32], H. Miyamoto[32], A. Santangelo[33], E. Kendziorra[33], F. Fenu[33], P. Biermann[34], K. Mannheim[35], J. Wilms[36], M. Focardi[37], E. Pace[37], P. Spillantini[37], V. Bratina[38], L. Gambicorti[38], A. Zuccaro[38], A. Anzalone[39], O. Catalano[39], M.C. Maccarone[39], P. Scarsi[39], B. Sacco[39], G. LaRosa[39], G. D'Ali Staiti[40], D. Tegolo[40], M. Casolino[41], M.P. De Pascale[41], A. Morselli[41], P. Picozza[41], R. Sparvoli[41], P. Vallania[42], P. Galleotti[43], C. Vigorito[43], M. Bertaina[43], G. Osteria[44], D. Campana[44], G. De Rosa[44], M. Ambrosio[44], C. Aramo[44], F. Isgro[45], S. Russo[45], D. D'urso[45], F. Guarino[45], G. Medina-Tanco[46], J.C. D'Olivo[46], J.F. Valdes[46], H. Salazar[47], O. Martines[47], L. Villasenor[48], S. Nam[49], I.H. Park[49], J. Yang[49], J.H. Park[49], T. Chung[49], T.W. Kim [50], S.W. Kim [51], K.K. Joo [52], G.K. Garipov[53], B.A. Khrenov[53], P.A. Klimov[53], M.I. Panasyuk[53], I.V. Yashin[53], D. Naumov[54], L. Tkachev[54], A. Maurissen[55], V. Mitev[55], D. Rodriguez-Frias[56], L. Peral[56], J. Gutierrez[56], R. Gomez-Herrero[56]
(The JEM-EUSO collaboration)

[a] Corresponding author: sakaki@phys.aoyama.ac.jp

[4] Aoyama Gakuin University, 5-10-1 Fuchinobe, Sagamihara, Kanagawa 229-8558, Japan,
[1] RIKEN, Japan, [2] Konan University, Japan, [3] Fukui University of Technology, Japan,
[5] Saitama University, Japan, [6] National Institute of Radiological Sciences, Japan, [7] University of Tokyo, Japan,
[8] Tohoku University, Japan, [9] Institute for Cosmic Ray Research (ICRR), University of Tokyo, Japan,
[10] High Energy Accelerator Research Organization (KEK), Japan, [11] Chiba University, Japan,
[12] National Astronomical Observatory of Japan, [13] Tokyo Institute of Technology, Japan
[14] Institute of Space and Astronautical Science(ISAS), Japan Aerospace Exploration Agency(JAXA),
[15] Kanazawa University, Japan, [16] Nagoya University, Japan,
[17] Solar-Terrestrial Environment Laboratory, Nagoya University, Japan,
[18] Yukawa Institute for Theoretical Physics, Kyoto University, Japan, [19] Kyoto University, Japan,
[20] Kobe University, Japan, [21] Japan Atomic Energy Agency (JAEA) [22] Kinki University, Japan,
[23] Hiroshima University, Japan, [24] Hokkaido University, Japan, [25] Marshall Space Flight Center(MSFC), NASA, USA,
[26] University of Alabama in Huntsville, USA, [27] E. O. Lawrence Berkeley National Laboratory, USA,
[28] University of California, Los Angeles, USA, [29] Vanderbilt University, USA, [30] University of Arizona, USA,
[31] APC Laboratory, University of Paris, France, [32] Max Planck Institute for Physics, Germany,
[33] University of Tuebingen, Germany, [34] Max Planck Institute for Radio Astronomy, Germany,
[35] University of Wuerzburg, Germany, [36] University of Erlangen, Germany, [37] University of Firenze, Italy,
[38] National Institute of Applied Optics, Italy, [39] IASF Palermo, National Institute for Astrophysics(INAF), Italy,
[40] University of Palermo, Italy, [41] INFN and University of Rome "Tor Vergata", Italy,
[42] Institute of Physics of Interplanetary Space, National Institute for Astrophysics, Italy,
[43] University of Torino [44] National Institute of Nuclear Physics(INFN), Napoli, Italy,
[45] University of Napoli Federico II, Italy, [46] UNAM, Mexico, [47] BUAP,Mexico, [48] UMSNH, Mexico,
[49] Ewha Women University, Republic of Korea, [50] Ajou University, Republic of Korea,
[51] Yonsei University, Republic of Korea, [52] Chonnam National University, Republic of Korea, [53] SINP MSU, Russia,
[54] Dubna JINR, Russia, [55] Neuchatel Observatory, Switzerland, [56] University of Alcala, Spain

Abstract— **Extreme Universe Space Observatory (EUSO) is a mission to study ultra-high energy phenomena in the Universe. Ultra-high energy cosmic rays (UHECRs) above $\sim 10^{20}$eV will be observed by a super-wide field of view ($\pm30^\circ$) telescope with 2.5 meter in diameter attached to the International Space Station. The requirement is observation of more than 1000 UHECRs above 7×10^{19} eV, which is necessary statistics for astronomy with ultra-high energy particles. In this paper, the structure of the JEM-EUSO telescope will be described. Expected performance and recent improvements will be also reported.**

I. INTRODUCTION

About a half century has passed since the first 10^{20}eV cosmic ray had been observed[1], however, the origin of cosmic rays above 10^{20}eV has not been identified. A proton above the energy of 4×10^{19}eV interacts with the microwave background radiation and looses its energy to produce pions[2], [3]. Therefore the origin should be in the local universe, within $\sim$50 Mpc. Nuclei such as iron and gamma ray at 10^{20}eV interact with background radiation to loose their energy, so that the attenuation lengths are similar to that of proton or shorter. Recent results by the HiRes experiment[4] and the Pierre Auger Observatory[5] shows possible suppression in the energy spectrum by GZK mechanism[6], [7]. So far, astrophysical sources to accelerate particles up to 10^{20}eV have not been found within 50 Mpc. However, the cluster events of UHECR observed by AGASA suggests point sources[8] and the correlation between the arrival direction distribution of UHECR and the distribution of local active galactic nuclei (AGNs) was reported by the Auger group[9]. They have not been confirmed yet mainly due to the limited statistics.

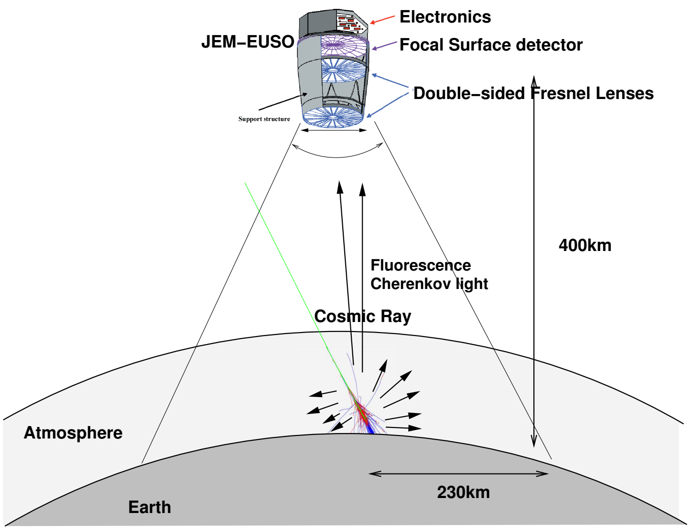

Fig. 1. Observation of cosmic rays by the JEM-EUSO telescope. It is attached to the JEM/EF of ISS at 400 km in height to see towards the Earth.

JEM-EUSO is a mission that a super-wide-angle telescope with 2.5 meter in diameter is attached to the Japanese Experiment Module Exposure Facility (JEM/EF) of the International Space Station (ISS) and views the Earth atmosphere (Figs.1 and 2). A UHECR goes into the atmosphere and induces an extensive air shower (EAS), which consists of a lot of electrons. These electrons excites Nitrogen in the atmosphere and fluorescence is produced in the wavelength of 300-450 nm. The fluorescence and Čerenkov light is detected by the telescope. A UHECR is observed as a bright point moving along a line with variation of intensity. Parameters such as the energy and the arrival direction will be determined from the intensity and the direction of the line. The field of view (FoV) of the telescope is very wide, $\pm30^\circ$, so that an area of about 50,000 km^2 will be seen at once. The whole sky will be covered by a single telescope since the ISS flies around the Earth. This is a big advantage to study the arrival direction distribution of UHECR, because comparison of different observations on ground requires understanding of systematic uncertainties. If there are several bright sources, energy spectrum for each source may be obtained and astronomy with UHECR will start[13].

EUSO was originally selected in 2000 as a mission of the European Space Agency (ESA). The Phase A study was completed successfully in 2004, but the start of Phase B was postponed due to the financial trouble in Europe. It was reconstructed as the JEM-EUSO mission by Japanese and USA team to utilize the JEM/EF. In 2006, JEM-EUSO was accepted as a mission candidate of the second phase of JEM/EF utilization and the Phase A study has started. After the ESA Phase A study, the energy threshold has been decreased by new optics design with new lens material, detectors with higher quantum efficiency and improvements of the trigger algorithm. In the later phase of the mission, the telescope will be inclined to emphasize the observation of higher energy cosmic rays than 10^{20}eV (Fig.2). JEM-EUSO is planed to be launched by a H-IIB rocket in 2013 and be delivered to the ISS by a H-II Transfer Vehicle (HTV).

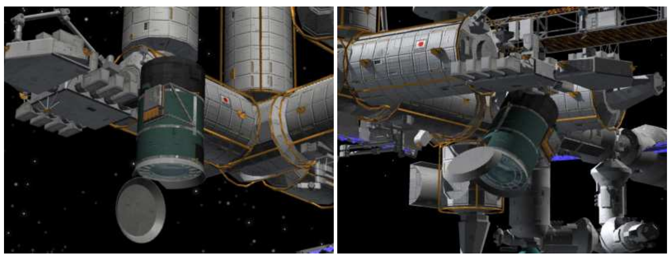

Fig. 2. Two operation modes of JEM-EUSO. The left picture shows nadir mode and the right one shows tilted mode.

This paper is focused on the description of the JEM-EUSO instrument and the science targets and the general information of the mission will be described in another paper[11].

II. INSTRUMENT

A. Overview

The JEM-EUSO telescope is divided into four parts: optics, focal surface, atmospheric monitor and calibration system (Fig.3) [14]. The optics consists of two Fresnel lenses with a diameter of 2.65 meter of which edges are cut by 1.9 meter in width, and a diffractive plate. Ultra violet (UV)

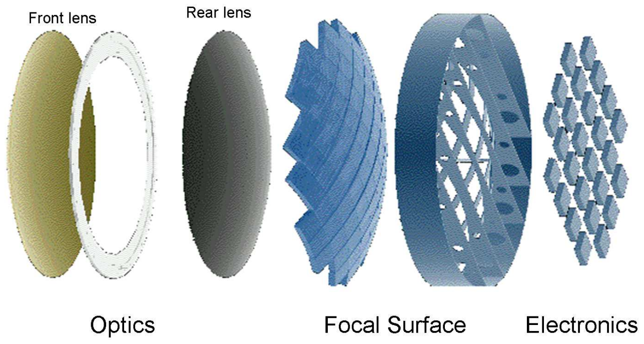

Fig. 3. The structure of the JEM-EUSO telescope.

light in 330–400 nm is collected to the focal surface with an angular resolution of 0.1 degree. The collected light is converted to electric signal by multi-anode photomultiplier tubes (MAPMTs). The electric pulses are counted every 2.5 μs and the number of signals is stored into a memory as a picture. If it is judged as a UHECR event, the information in the memory before and after the trigger time will be read and transferred to the ground. Since the observation target is phenomena in the atmosphere, the atmospheric condition should be monitored. It is done by a UV LIDAR (LIght Detection And Ranging) and an infrared camera to be used for analysis of cosmic rays. The change of the telescope performance with time and atmospheric transmittance will be checked regularly by UV LEDs on board and by UV flasher lamps on ground.

B. Optics

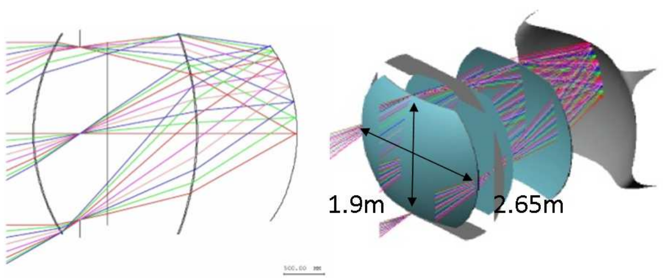

Fig. 4. The design of the optics. It consists of two Fresnel lenses and diffractive plane between them. The F number is 1.

In order to realize an optics with super wide angle FoV and light weight, optics with two double-sided Fresnel lenses made of UV transparent material and one diffractive lens is adopted for JEM-EUSO[15]. Fig.4 shows a drawing of the optics. It is designed to optimize the performance for the light in 330-400 nm. The angular resolution is 0.1 degree, which corresponds to 0.8 km on ground observed from the height of 430 km. The lens material is an amorphous fluorinated resin, CYTOP (Asahi Glass Co., Ltd). CYTOP has a transparency of larger than 95% above 300 nm, while the transparency of PMMA, which was a lens material in the past design, starts to decrease around 350 nm and down to 80% at 300 nm. Another advantage of CYTOP over PMMA is a low dispersion of the refractive index, which leads to less chromatic aberration. A little residual chromatic aberration is reduced by the diffractive lens between the Fresnel lenses. In total, the light collection power has increased by a factor of 1.5 to ESA EUSO optics. In the current design, the two Fresnel lenses with 2.65 meter in diameter are cut with 1.9 meter in width[12]. The light collection power is same as for a full-circled lens with 2.5 meter in diameter for the light incident parallel to the light axis. At surrounding parts of the FoV, it is decreased by about 10% because some rays were supposed to pass through the cut area. The manufacturing precision for a small piece satisfies the requirement of surface roughness, $<$20 nm RMS. We are now preparing for machining larger lenses, whose diameter is $>$1.5 meter in RIKEN. The first lens will be made in several months and the machining precision will be evaluated.

C. Focal Surface Detector

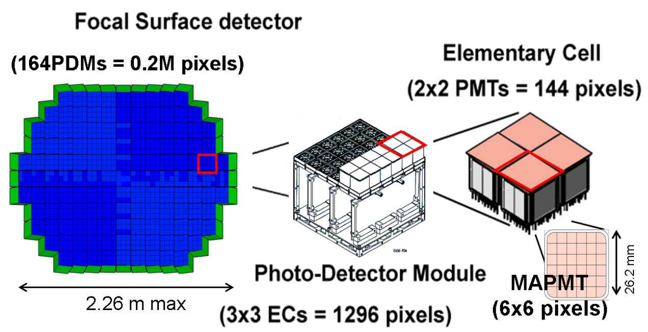

Fig. 5. Hierarchical structure of the focal surface detector.

The focal surface consists of 2×10^5 pixels in total of MAPMTs (Fig.5)[16]. Four MAPMTs compose Elementary Cell (EC), which is the smallest unit for signal processing and the first trigger. Nine ECs make a Photo-Detector Module (PDM), which is a unit for the data acquisition. A PDM works independently, and have functions to judge whether an event is a possible EAS data or not. The used MAPMT is R8900-03-M36 (Hamamatsu Photonics) with 6×6 pixels, developed for EUSO. Photo-electrons are focused on the first dinode by a weak electric field to make the effective detection area larger. Fundamental evaluation was already completed in the phase A study of ESA EUSO[18]. At that time, typical quantum efficiency (Q.E.) was about 25%. Recently Hamamatsu has succeeded to increase Q.E. up to about 40% (Ultra-Bialkali photocathode). Several R8900-03-M36 PMTs with Ultra-Bialkali photocathode were manufactured in trial and the photon detection efficiency (D.E.:=Q.E.$\times$C.E.) was measured. It was found to be about 30%, which is 1.5 times better than a MAPMT with normal bialkali photocathode. Since expected number of photons at the EUSO telescope is small, SiPM detector is considered to be used as a possible focal surface detector, which has better Q.E. than PMTs. The development is on going in German, Russia and Japan, however, operation as a multi-pixel array and stability in the JEM-EUSO environment should be studied further to adopt it.

D. Electronics and Trigger Algorithm

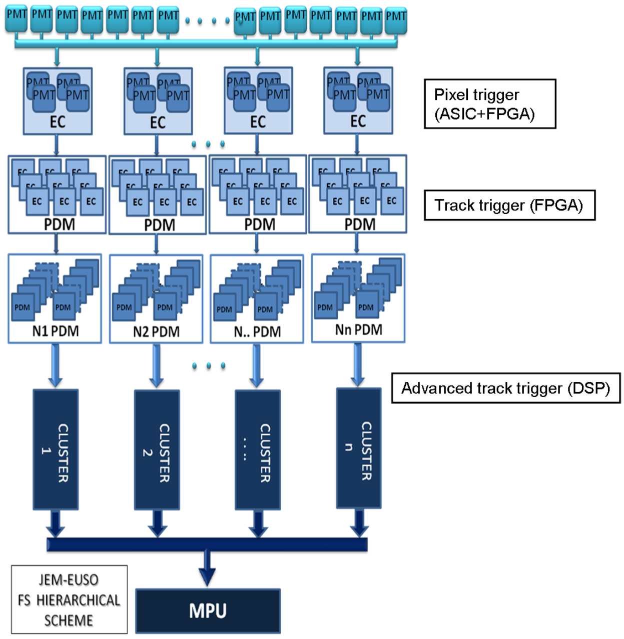

Fig. 6. Hierarchical scheme of the data stream and trigger system.

The data acquisition circuit and the trigger have a hierarchical structure with three layers as shown in Fig.6[12], [17]. Operation modes are main one for UHECR observation, slow mode for Transient Luminous Events(TLEs) and meteorites, fast mode for LIDAR and calibration mode. The gate time unit(GTU) of the photon counting for each mode is 2.5 μs for UHECR observation, 40 μs for slow mode and 0.156 μs. Data are reduced by three stages of trigger to satisfy the transmission rate to ground, 300 kbps.

EC includes front-end ASIC(s) and FPGA(s). Charge from a MAPMT anode is converted to a square pulse with time width proportional to the charge (Q-T conversion) by a front-end ASIC. The pulse width is counted with a clock pulse by the front-end FPGA. This ASIC+FPGA system is designed to work at single photo-electron level ($\sim 5 \times 10^5 e$) and the counted pulse width corresponds to the number of incident photons. The count is sent to a ring buffer in a corresponding FPGA in the PDM every GTU for the second trigger judgment. The Q-T conversion has an advantage over the usual photon counting method that it consumes less power and that count loss is avoidable if many photons come at once.

We have already made the ASIC in trial and confirmed that 1) The power consumption was 1.8mW/ch as designed, 2) linearity up to 300 p.e. level and 3) various functions implemented in the chip worked. The total power for the whole telescope is limited to ~1 kW, so that we have designed ASIC with much less power consumption, 0.7mW/ch. The trial pieces will be delivered by March, 2009.

There are two threshold levels for each pixel, $N_{th;r}$ and $N_{th;y}$ ($N_{th;r} > N_{th;y}$). The pixel whose count, N, is larger than $N_{th;r}$ is called *red pixel*, the pixel with $N > N_{th;y}$ is called *yellow pixel* and the other is called *white pixel* which is not used in the trigger algorithm. These threshold counts will be adjusted according to the background level in observation. The second level trigger in FPGA is to find a track moving at the speed of light along a specific line. This algorithm is called Track Trigger Algorithm (TTA). First, a red pixel is searched. If it is found, the number of photo-electrons are integrated for the red and yellow pixels within ±4-5 GTU centered at the red pixel along a specific direction. The directions are predefined for 16 directions at present. If the summed number of photo-electrons go beyond a certain threshold level (N_{th}), a second level trigger will be issued. The threshold levels, N_{th}, $N_{th;r}$ and $N_{th;y}$ depends on the average background level and are set so that the trigger rate is between 0.1 Hz and 1000 Hz at present.

The data will be sent to a cluster control board equipped with digital signal processors (DSPs) for the third level trigger. The algorithm of the third level trigger is essentially same as the second one, but the event will be examined in more detail and events across over PDMs will be also checked for trigger.

At last, events judged as EAS events will be handled by mission data processors (MDPs) and will be sent to ground by way of the ISS interface together with house keeping data.

The electronics is required to work in stable in the space (ISS) environment. The JEM-EUSO electronics is based on those for Pamela, Agile, Altea and Sileye-3, which works successfully in space, and incorporates new technologies for recent CPUs and FPGAs to match the JEM-EUSO data acquisition system.

E. Atmospheric monitoring

As described above, JEM-EUSO observes light emitting phenomena in the atmosphere. Therefore it is important to obtain the atmospheric conditions during the UHECR observation. Information on the cloud is necessary especially for analysis of low energy events around threshold energy with better quality and for the estimation of the exposure. In order to measure the vertical structure (height) of clouds, third harmonics (355 nm) of a 20 mJ Nd:YAG laser is shoot toward the atmosphere, at a few directions[19]. Scattered light is received by the JEM-EUSO telescope to reduce the power. Intensity of the scattered light is taken every 0.156 μs with the fast mode and then vertical distribution of clouds will be obtained. In addition to the LIDAR, the FoV of the JEM-EUSO telescope is monitored with an infrared camera (10-12μm) with the similar FoV to obtain the distribution of cloud top height[19].

F. Calibration

The energy of a cosmic ray is essentially proportional to the amount of detected light. In order to determine the intensity of the shower maximum in the EAS development, it is required to determine the emitted amount of light accurately. Therefore it is necessary to know attenuation and conversion factors between the source and the detector. Calibration works in flight for JEM-EUSO are classified into three parts[12].

Three kinds of LEDs in the range of 330-400nm are put on the back side of the rear lens to illuminate the focal surface detectors directly in the days. The variation of the efficiency in time will be checked with it. If any change is found, high voltage or threshold levels will be adjusted. LED light source is put on the focal surface and illuminate through the lenses. The reflected light at the rear side of the lid is detected by the focal surface detectors. This data is used to check the transmittance of the optics.

Second one is 10-20 stations of Xe flashers on ground, whose intensity are calibrated[20]. JEM-EUSO will fly over one of the flashers once per day. The transmittance of the atmosphere and the degradation of light collection power of the telescope and of the light detection efficiency will be checked.

UV LIDAR (355nm) is used to emulate EASs and evaluate the precision of energy determination and angular determination. Some LIDAR stations will be settled on the same place as a flasher to cross-calibrate the vertical transmittance of the atmosphere.

III. EXPECTED PERFORMANCE

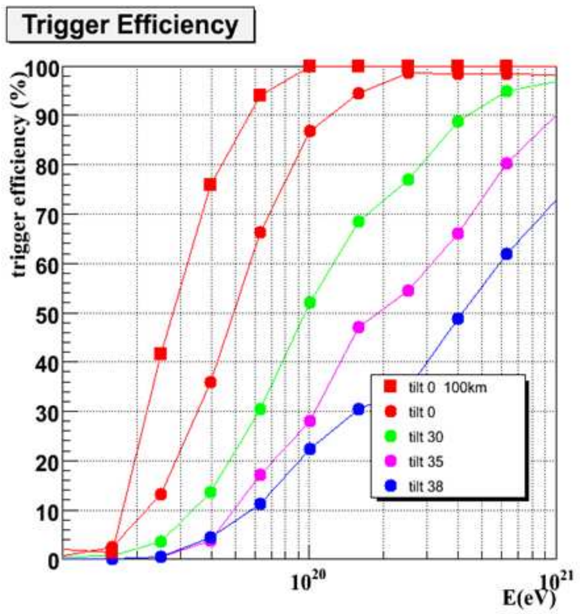

Fig. 7. Trigger efficiency as a function of primary cosmic ray energy. The efficiency of the full FoV is shown by circles for four kinds of tilt angles (0, 30, 35 and 38°) and that for the center area of the FoV is shown by squares.

The performance of the JEM-EUSO was evaluated by simulation. First, EAS data base was made. Then fluorescence and Čerenkov light is calculated for each EAS and the information of the photons (position, direction, time, wavelength, etc.) arrived at the entrance of the telescope at 430 km in height is recorded taking account of attenuation in the atmosphere. In the detector simulation, characteristics of the optics, efficiency of the PMTs, electronics, etc. are taken into account to produce simulated event sets. They are reconstructed and the performance was evaluated. In the calculation, the background light intensity was assumed to be 500 photons/m^2·ns·sr. Fig.7 shows the trigger efficiency as a function of energy. If the trigger threshold is defined as the energy where 50% of events in the FoV are triggered, it is 5×10^{19} eV for the nadir mode. In the later phase of the mission, the telescope will be inclined to increase the covered area especially at higher energy than 10^{20}eV. The trigger efficiency at 10^{20}eV is smaller than in the nadir mode. However covered area on ground is three times larger at 35° in nadir angle and about five times larger at 38°. Beyond 38°, the telescope starts to see the sky above the horizon. Therefore it is more appropriate to see

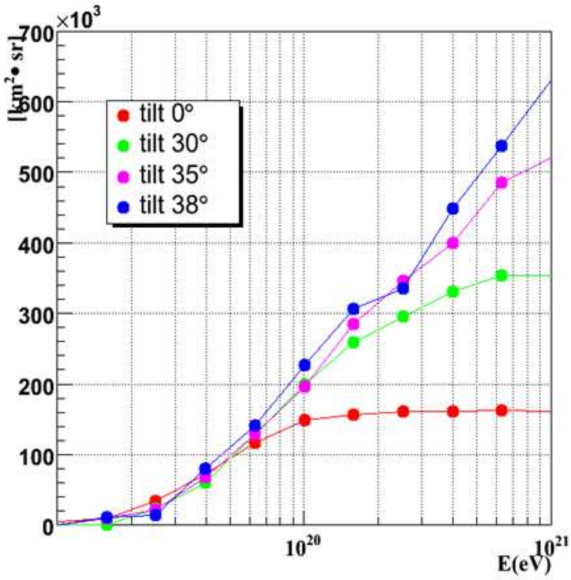

Fig. 8. Effective area as a function of energy for four kinds of tilt angles (0, 30, 35 and 38°).

the effective detection area in order to show the detection power. It is shown in Fig.8 assuming the duty cycle of 19%. The area for the nadir angle of 38° starts to become larger than in the nadir mode from below 10^{20} eV, and it is 1.8 times larger at 10^{20} eV and 2.4 times larger at $10^{20.5}$ eV. Expected number of events during the 5-year mission period, with the nadir mode for 2 years and with the tilt mode (38 deg.) for 3 years, was calculated. The energy spectrum was normalized to the Auger's result as $J(E)E^3 = 2.0 \times 10^{24}$ [(eV)^2/m^2·s·sr] at 2×10^{19} eV. 1800 events above 7×10^{19} eV, which satisfies the requirement, and 450 events above 10^{20} eV are expected. For the events below the threshold energy, the full trigger efficiency is worse but more than 1000 events per year are expected around 3×10^{19} eV even if only the events at the center of the FoV, with the radius of the area on ground less than ∼100 km where the efficiency is good, because of steep energy spectrum slope are used. It is enough statistics for the study of anisotropy and comparison of the energy spectrum with the results of ground experiments. The energy resolution and the angular resolution are less than 30% and less than 2.5° respectively for events with zenith angle larger than 45° at 10^{20} eV. The angular resolution for the events with zenith angle larger than 60° is $\sim$1 degree, which will be powerful for search of sources. The resolution of the shower maximum depth ($X_{\rm max}$) is about 120 g/cm^2 and it is capable to discriminate ultra-high energy neutrinos.

IV. SUMMARY

EUSO was reconstructed as JEM-EUSO and was accepted as a mission candidate of the second phase of JEM/EF utilization in 2006. The main science target is astronomy with ultra high energy particles around and above 5×10^{19} eV. The performance of JEM-EUSO telescope has been improved by adoption of the CYTOP optics, high detection efficiency MAPMT and more intelligent trigger algorithm. About 1800 events are expected during the 5-year mission period above 7×10^{19} eV. In this energy region, deflection by galactic and intergalactic magnetic field is small and identification of UHECR sources will be promising.

ACKNOWLEDGMENT

This work is supported in part by a grant-in-aid for scientific research No. 19740147 from the ministry of education, culture, sports, science and technology, Japan.

REFERENCES

[1] J. Linsley, Phys. Rev. Lett. **10** (1963) 146.
[2] K.Greisen, Phys. Rev. Lett. **16** (1966) 743.
[3] G.T.Zatsepin and V.A.Kuz'min, JETP Lett. **4** (1966) 78.
[4] S.C.Corbato *et al.*, Nucl. Phys. B (Proc. Suppl.) **28B** (1992) 36.
[5] J. Abraham *et al.* (Pierre Auger Collaboration), Nucl. Instr. Meth. A **523** (2004) 50.
[6] P. Sokolsky and G.B. Thomson (The HiRes collaboration), Nucl. Phys. (Proc. Suppl.), **175-176** (2008) 207.
[7] J. Abraham *et al.* (Pierre Auger Collaboration), Phys. Rev. Lett. **101** (2008) 061101.
[8] N. Hayashida *et al.* (The AGASA collaboration), Astrophys. J., **522** (1999) 225; Y. Uchihori *et al.*, Astropart. Phys., **13** (2000) 151.
[9] J. Abraham *et al.* (The Pierre Auger Collaboration), Science **318** (2007) 938.
[10] T. Ebisuzaki *et al.* (The JEM-EUSO collaboration), Proc. of 30th Int'l Cosmic Ray Conf. (Merida), (2007); `http://jemeuso.riken.jp/`
[11] P. Gorodetzky *et al.* (The JEM-EUSO collaboration), in this workshop proceedings (2008).
[12] The JEM-EUSO collaboration, The Phase-A research report of the JEM-EUSO mission, (2008).
[13] Y. Takahashi *et al.* (The JEM-EUSO collaboration), Proc. of 30th Int'l Cosmic Ray Conf. (Merida), (2007).
[14] F. Kajino *et al.* (The JEM-EUSO collaboration), Proc. of 30th Int'l Cosmic Ray Conf. (Merida), (2007).
[15] J.H. Adams *et al.* (The JEM-EUSO collaboration), Proc. of 30th Int'l Cosmic Ray Conf. (Merida), (2007).
[16] Y. Kawasaki *et al.* (The JEM-EUSO collaboration), Proc. of 30th Int'l Cosmic Ray Conf. (Merida), (2007).
[17] M.E. Bertaina *et al.* (The JEM-EUSO collaboration), Proc. of 30th Int'l Cosmic Ray Conf. (Merida), (2007).
[18] Y. Kawasaki, M.E. Bertaina, N. Sakaki *et al.* (The JEM-EUSO collaboration), Nucl. Instr. Meth. A **564** (2006) 378.
[19] V. Mitev *et al.* (The JEM-EUSO collaboration), Proc. of 30th Int'l Cosmic Ray Conf. (Merida), (2007).
[20] J.H. Adams *et al.* (The EUSO collaboration), Proc. of 28th Int'l Cosmic Ray Conf. (Tsukuba), (2003) 919.